Available online at www.sciencedirect.com

ScienceDirect

Advances in Space Research xxx (xxxx) xxx

ADVANCES IN SPACE RESEARCH (a COSPAR publication)

www.elsevier.com/locate/asr

Simulation and mapping of drought and soil erosion in Central Yunnan Province, China

Yuanhe Yu [a,c,d], Yuzhen Shen [a,c,d], Jinliang Wang [b,*], Yuchun Wei [a,c,d,*], Zhiyuan Liu [e]

[a] School of Geography, Nanjing Normal University, Nanjing 210023, China
[b] Faculty of Geography, Yunnan Normal University, Kunming 650500, China
[c] Jiangsu Center for Collaborative Innovation in Geographical Information Resource Development and Application, Nanjing 210023, China
[d] Key Laboratory of Virtual Geographic Environment (Nanjing Normal University), Ministry of Education, Nanjing 210023, China
[e] Institute of Meteorological Science of Qinghai Province, Xining 810001, China

Received 2 February 2021; received in revised form 10 August 2021; accepted 19 August 2021

Abstract

Central Yunnan Province is the political, economic, cultural, and transportation hub of Yunnan Province, China. Climate change has resulted in increased seasonality of global averaged precipitation, temperature, runoff, and evapotranspiration, thereby exacerbating extreme events such as drought and soil erosion. The simulation and mapping of drought and soil erosion within Central Yunnan Province is important for achieving sustainable development. This study constructed a comprehensive drought monitoring model and a soil erosion model based on multiple sources of remote sensing data, considering numerous drought and soil erosion factors. The temporal and spatial characteristics of dry-season drought and soil erosion for 2010 to 2018 in Central Yunnan Province were explored, and the extents of soil erosion in different parts of Central Yunnan Province were quantified using the soil erosion intensity index. The results showed that: (1) The multi-year average percentage dry-season drought coverage and average drought frequency were 33.98% and 18.33 months, respectively. Although drought frequency was higher in areas with high drought intensity, dry-season drought showed a long-term weakening trend. (2) Over the study period, the multi-year average soil erosion of Central Yunnan Province was 1,551.45 t km^{-2}·yr^{-1}. Soil erosion showed an initial overall increasing trend, followed by a decreasing trend, dominated by micro erosion, mild erosion, and moderate erosion, whereas the mountains and valleys in north and southwest parts of Central Yunnan Province experienced severe erosion. Vegetation coverage and slope were identified as the main factors driving soil erosion. (3) The soil erosion intensity index was a good indicator of soil erosion severity across different spatial scales and different drought grades. The soil erosion intensity index showed a positive relationship with drought grade. The correlation coefficients between soil erosion intensity and drought frequency and between soil erosion intensity and drought intensity were 0.2623 and −0.2679, respectively. This study demonstrated that drought affects soil erosion and that water and soil conservation measures such as afforestation and vegetation greening are beneficial to mitigating soil erosion and drought in Central Yunnan Province.

Keywords: Comprehensive drought index; Soil erosion; Soil erosion intensity index; Climate change; Central Yunnan Province

1. Introduction

Climate change has altered the frequency of the hydrological cycle, resulting in increases in global average precipitation, runoff, and evapotranspiration (Kourgialas, 2020). Consequently, climate events such as droughts and

* Corresponding authors at: Faculty of Geography, Yunnan Normal University, Kunming 650500, China (J. Wang); School of Geography, Nanjing Normal University, Nanjing 210023, China (Y. Wei).
E-mail addresses: jlwang@ynnu.edu.cn (J. Wang), Weiyuchun@njnu.edu.cn (Y. Wei).

https://doi.org/10.1016/j.asr.2021.08.028
0273-1177/

floods are becoming more frequent and extreme (Konapala et al., 2020; Shao and Kam, 2020). Drought broadly refers to persistent water deficits over land (Shao and Kam, 2020) and long-term drought can result in crop failure, food shortages, famine, land degradation, and other social and environmental problems (Jiao et al., 2019). Drought is regarded to be the most complex and destructive category of natural disaster globally (Javed et al., 2020). Soil erosion is a process of soil migration under specific spatiotemporal scales (Lee et al., 2020) and is considered among the most serious environmental challenges facing humanity (Wang et al., 2019). Soil erosion is exacerbated by the frequency of natural disasters such as floods and droughts, whereas severe soil erosion can worsen the ecological environment, thereby promoting the occurrence of droughts and floods (Zhang et al., 2016). Therefore, soil erosion has a direct causal relationship with droughts and floods. In addition, drought and soil erosion exacerbated by climate change result in environmental, economic, and social challenges at a global level (Zhang et al., 2016).

The frequency and intensity of droughts have increased globally in recent decades (Liu et al., 2021; Wang et al., 2020). This trend has been linked to increases in water demand and the complex changes in hydrological and climatic factors (Balti et al., 2020; Jehanzaib et al., 2020). Quantifying drought severity remains a challenge as drought severity cannot be measured directly (Santos et al., 2021). Consequently, meteorological drought and remote sensing indices have become the most widely used drought monitoring methods (Yu, 2020). Due to their maturity and high accuracy, meteorological drought indices are widely used for drought analysis across multiple temporal scales (Santos et al., 2021; Yao et al., 2018). Drought indices include the standardized precipitation index (SPI) (McKee T B et al., 1993) and the standardized precipitation evapotranspiration index (SPEI) (Vicente-Serrano et al., 2010). However, drought analysis through interpolation methods generally does not reflect spatial changes (Yu et al., 2020). Remote sensing methods have diversified since the 1970s, and single indices such as the vegetation condition index (VCI) (Kogan, 1990), temperature condition index (TCI) (Kogan, 1995), and tropical rainfall condition index (TRCI) (Yu and Wang, 2020) are widely used in remote sensing-based drought monitoring. However, the results of drought monitoring are not comprehensive and suffer from time lags when only focusing on a single aspect, such as soil or vegetation (Shen et al., 2019). Therefore, many studies have considered a variety of factors for the construction of a comprehensive drought model (Ji et al., 2018; Yu et al., 2019). For example, the vegetation health index (VHI), constructed through an integration of VCI and TCI, achieved drought monitoring results that were closer to the actual drought situation compared to that achieved through the use of a single index (Bento et al., 2018). However, precipitation is one of the factors affecting regional drought that has not been considered within a comprehensive drought index, and the integration of precipitation, VCI, TCI, and other factors within the construction of a comprehensive drought model can improve the monitoring of the complex process of drought evolution (Ji et al., 2018).

The increased frequency in drought as a consequence of climate change has resulted in the aggravation of soil erosion rates (Ciampalini et al., 2020). Traditional soil erosion estimation is mainly based on small areas or runoff experiments (Li et al., 2011). Although studies using these traditional estimation methods achieved highly accurate results, these methods have several disadvantages, include difficulty in acquiring data and expensive testing and analysis (Li et al., 2011). Therefore, it is difficult and costly to apply these traditional approaches to large-scale regions (Safwan et al., 2021; Teng, 2017). Soil erosion models are the most extensive and effective methods for quantitatively studying research soil erosion. Among these models, the empirical statistical soil erosion models include the Universal Soil Loss Equation (USLE) and the Revised USLE (RUSLE) (Wischmeier and Smith, 1965). Many studies have improved and perfected soil erosion models based on these equations in combination with local soil erosion conditions. For example, Kebede et al. (2021) estimated soil loss at a watershed level using the RUSLE coupled with a geographic information system (GIS) tool. Qin et al. (2018) modified the RUSLE by adding a parameter representing the effective contribution of the existing slope length to construct a new soil erosion model (RUSLE-L). Rajbanshi and Bhattacharya (2020) combined the RUSLE with sediment delivery ratio models to generate spatial dimensions of soil erosion and specific sediment yields in Konar River Basin, India. Although the RUSLE was developed based on soil erosion experiments for catchments in the United States, some studies have investigated the adaptability of the RUSLE parameters for different geomorphic features (such as karst, mountains, and hilly and intricate plateau regions) (Gao and Wang, 2019; Jin et al., 2021; Li et al., 2019), different land use types (Almohamad, 2020; Wu et al., 2021), different soil types (Bircher et al., 2019; Huang et al., 2019), different slopes (Zhao et al., 2021), and different countries and climatic regions (Gharibreza et al., 2021; Pal and Chakrabortty, 2019; Prasannakumar et al., 2011; Teng et al., 2019). These studies demonstrated that the RUSLE model achieved good performance. Therefore, the current study applied the RUSLE model to Central Yunnan Province to estimate the soil erosion.

Yunnan Province forms the southwest border of China, and is known to experience frequent natural disasters due to its complex topography, remarkable stereoscopic climate, extensive distribution of karst landform, and unique geological structure (Zhou and Yang, 2013). Central Yunnan Province is the economic hub of Yunnan Province, and includes the cities of Kunming, Yuxi, and Qujing and Chuxiong Prefecture (Yu et al., 2014). Central Yunnan Province is also positioned in a focal point of disasters in the province and may

experience both drought and soil erosion within a single year. At the same time, the economic development of Central Yunnan Province is related to the development of Yunnan Province and Southwest China. Previous studies on drought or soil in Central Yunnan Province have focused on individual disasters (Javed et al., 2020; Liu et al., 2020; Nepal et al., 2021; Yu et al., 2020). However, drought and soil erosion have a certain causal relationship. For example, soil erosion changes the hydraulic and physical properties of soil, and such changes will in turn, influence the infiltration of rainwater and surface runoff and thus, increase the likelihood of soil drought (Li et al., 2021). Sidiropoulos et al. (2021) indicated that extended drought periods may cause soil exposure and erosion and the degradation of land. Santra and Santra Mitra (2020) observed that the mean rate of soil loss for the areas in which drought is very frequent is almost double that of the areas in which the frequency of drought is very low. Studies on the relationship between soil erosion and drought in Central Yunnan Province remain limited. For example, Jia and Lu (2012) found that owing to the destruction of forests and wetland ecosystems in Yunnan Province, there is no conserved water to apply in the dry season, and soil erosion frequently occurs during the rainy season, resulting in the deposition of sediment in reservoirs, a reduction in effective storage capacity, and a reduction in the ability to store water. However, the relationship between drought and soil erosion has not been described.

Therefore, the present study aimed to simulate and map drought and soil erosion in Central Yunnan Province to identify the relationship between soil erosion and drought. The results of the present study can contribute to the assessment of risks of natural disaster and can contribute to soil conservation. The objectives of the current study were to: (1) evaluate and plot the spatial distribution of drought in Central Yunnan Province through analyzing drought intensity, drought frequency, and change in drought from 2010 to 2018; (2) simulate and analyze soil erosion in Central Yunnan Province for 2010, 2015, and 2018 through the use of the RUSLE, and; (3) use the soil erosion intensity index to analyze soil erosion in different counties and under different drought grades.

2. Study area

Central Yunnan Province is the economic hub of Yunnan Province and is located between 100°43′–104°50′E and 23°19′–27°03′N, with a total area of 94,558 km^2 (Fig. 1). Central Yunnan Province is dominated by mountains and inter-mountain basins with a gentle terrain and a mid-subtropical monsoon climate. The temperature of Central Yunnan Province decreases with altitude. The region has a remarkable stereoscopic climate with distinct dry and wet seasons. The dry season extends from November to April of the following year, and only accounts for 15% of annual precipitation. Therefore, this region tends to experience frequent droughts. The rainy season extends from May to October and shows an uneven spatial distribution of rainfall. Central Yunnan Province tends to experience regional heavy rainfall events or single rainstorm events that contribute to soil erosion. For example, Yunnan Province has suffered severe one in 100-year drought disasters during autumn, winter, spring, and early summer since the autumn of 2009, which has affected half of the population of the province and has reduced spring grain production by 50%. At the same time, the number of isolated rainfall events in the province during the flood season of 2010 decreased compared to that of the same period in previous years, although the intensity of rainfall was higher. The intensities of heavy rainfall events recorded at some sites in Central Yunnan Province, including at Malong, Songming, and Chenggong, all exceeded the historical maximums, and the rainfall was concentrated over relatively short periods, resulting in severe soil erosion (Zhao and Huang, 2012).

The dominant types of forest vegetation in Central Yunnan Province include evergreen broad-leaved forests, deciduous broad-leaved forests, and Yunnan pine forest, with an overall collective coverage rate of $\sim$ 53.8%. The strata in Yunnan Province are well developed, which has exposed layers from the Proterozoic to Quaternary (Zhang, 2020). The main stratigraphic lithologies are as follows. (1) The Cenozoic is primarily composed of continental sandstone, argillaceous sediments, and local intercalation of lignite or peat. It includes glutenite, fine silt, clay, sandy clay with lignite and clay with peat in the Quaternary, as well as trachyte, tuff, sandstone, coarse sandstone, shale, limestone and basalt in the Tertiary. The rocks described above are soft, have weak resistance to weathering and corrosion, and are mostly broken and loose. Therefore, they are easily stimulated by the external environment and can easily induce geological disasters, such as landslides and mudslides. (2) The Mesozoic is dominated by continental sandstone and mudstone. In particular, marl, sandstone, limestone, and purple-red shale intercalated with basalt in the Jurassic, are primarily distributed in Central Yunnan Province. (3) The Paleozoic is dominated by marine carbonate rocks and intercalated marine and continental clastic rocks. (4) The Proterozoic primarily includes dolomitic sandstone and quartz sandstone in the Sinian. In addition, due to its unique geotectonic setting, Central Yunnan Province contains strongly developed faults and folds. For example, geological disasters appear to be concentrated along the Xiaojiang, Puduhe, Luoci-Yimen, Yuanmou-Lvjujiang, Muding, and Xuanwei fault zones and along other active faults and nearby fold development zones (Ding et al., 2011). The soil types of the region are mainly Calcic Vertisols, Haplic Alisols, Haplic Acrisol, and Haplic Luvisol (WRB, 2014). Although these soils have high water permeability and can accommodate higher amounts of atmospheric precipitation, they have low water storage

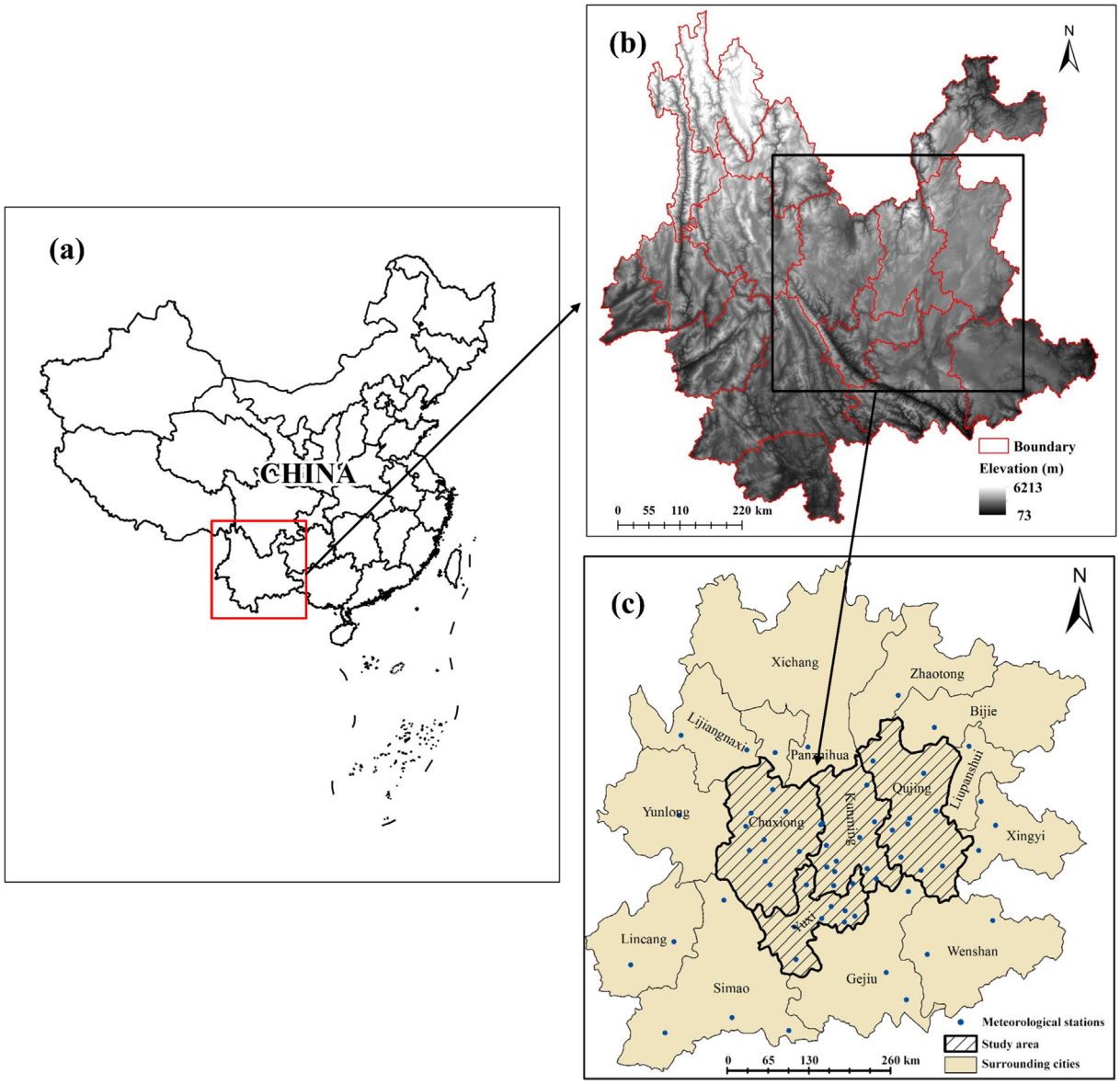

Fig. 1. The geographical location of Central Yunnan Province: (a) Map of China showing the position of Yunnan Province, (b) a digital elevation model (DEM) of Yunnan Province, and (c) the distribution of meteorological stations in Central Yunnan Province and surrounding cities.

and effective reservoir capacities and poor water retention. As a result, agriculture in these areas is vulnerable to drought (Ding et al., 2018).

3. Materials and methods

3.1. Data

Yunnan Province suffered not only a severe drought during 2010, but also severe geological disasters, with Central Yunnan Province particularly affected. Therefore, the starting point of the current study was November 2009, and remote sensing data and meteorological data were combined to study the dry-season drought and soil erosion conditions in Central Yunnan Province from 2010 to 2018.

3.1.1. Comprehensive drought monitoring data

Drought monitoring data obtained in the current study included: (1) Moderate Resolution Imaging Spectroradiometer (MODIS) remote sensing MOD11A2_LST data and MOD13A3_NDVI data, representing land surface temperature (LST) and the normalized difference vegetation index (NDVI), which were used to calculate the temperature condition index (TCI) and vegetation condition index (VCI), respectively. These indices were used as indicators within the construction of the comprehensive drought monitoring program. Since TCI assumes that drought events reduce soil moisture and result in surface thermal stress (Kogan, 1995), higher temperatures are regarded as a signal of drought. The VCI can compensate for the tendency of the NDVI to overestimate and

underestimate vegetation in low and high vegetation cover areas, respectively, and can reduce the influence of geographic and ecological factors other than moisture on the spatial variability of NDVI. (2) The current study used the Tropical Rainfall Measuring Mission (TRMM) 3B43 version 7 monthly data product obtained using TRMM multi-satellite precipitation analysis (TMPA), which was downscaled to a spatial resolution of 1 km × 1 km (Yu et al., 2020) to calculate the TRCI as one of the indicators for constructing the comprehensive drought monitoring program.

3.1.2. Soil erosion model data

The data collected in the current study for soil erosion modeling included: (1) Advanced Spaceborne Thermal Emission and Reflection Radiometer Global Digital Elevation Model (ASTER GDEM) data were used to calculate the slope length and steepness (LS) factor. (2) Landsat data were used for calculating vegetation cover, the management (C) factor, and the conservation practice (P) factor. (3) Monthly meteorological precipitation data from 65 meteorological stations were used to calculate the rainfall erosivity (R) factor. The above 65 meteorological stations consisted of 39 meteorological stations administered by Kunming City, Chuxiong Prefecture, Yuxi City, and Qujing City and 26 additional meteorological stations administered by the China Meteorological Data Service Center (http://data.cma.cn/). Among the meteorological station data used in the present study, precipitation data for each meteorological station extended from 20:00 to 8:00 and 8:00 to 20:00, and the data also included cumulative precipitation from 20:00 to 20:00. These daily precipitation data were accumulated to monthly. (4) Soil data used in the present study were based on the Harmonized World Soil Database version 1.1, obtained from the Cold and Arid Region Science Data Center (http://westdc.westgis.ac.cn). The soil data had a spatial resolution of 1 km × 1 km and were used to calculate the soil erodibility (K) factor. (5) Field survey data of land use types in 2018 were obtained for Chuxiong Prefecture (Shuangbai County), Yuxi City (Counties of Xinping, Tonghai, Huaning and Chengjiang), Kunming City (Xundian County) and Qujing City (Luoping County). In addition, the current study used a remote sensing-based survey of soil erosion status in Yunnan Province in 1999.

3.1.3. Elevation data

Basic geographic data were obtained from the ASTER GDEM V2 with a spatial resolution of 30 m × 30 m and were used to calculate the LS factor. Temperature and precipitation showed differences among the different elevations, thereby also affecting the conditions for drought (Zhang et al., 2017). Therefore, elevation data resampled to 1 km × 1 km was included as one of the driving factors for the construction of a comprehensive drought model.

3.2. Methods

3.2.1. Comprehensive drought monitoring model

Pearson proposed principal component analysis (PCA) for the study of random variables (Pearson, 1901). PCA has been applied in drought research with good results (Du et al., 2013; Mathbout et al., 2018). For example, Du et al. (2013) used PCA to correlate a comprehensive drought index constructed using VCI, TCI, and TRCI with SPI. This index improved the monitoring of meteorological drought while also maintaining the vegetation drought monitoring function of VCI and can also be used to monitor agricultural drought. However, while PCA considers the weight of information, it ignores the weight of importance of information within the subjective evaluation of the value of index weight coefficients. Saaty (1988) proposed the analytic hierarchy process (AHP), which has been shown to reasonably contribute prior knowledge to the evaluation process and has achieved good results in drought research (Han et al., 2016; Rahmati et al., 2020). However, AHP ignores the interrelationship between the indicators reflected by the objective data of the sample, and the error of subjective knowledge also impacts the accuracy of the results.

Therefore, the current study used precipitation, vegetation growth status, surface temperature, and elevation factors as indictors within the construction of the drought model. A comprehensive drought monitoring model for Central Yunnan Province was constructed by combining PCA and AHP, retaining the objective information of the sample, and integrating existing knowledge and experience to determine the weight coefficient of drought indicators.

The expression of the comprehensive drought index (CDI) is:

$$CDI_{ij} = \frac{1}{2}(PDI_{ij} + ADI) \quad (1)$$

$$PDI_{ij} = w_1 \times VCI + w_2 \times TCI + w_3 \times TRCI + w_4 \times DEM \quad (2)$$

$$ADI = 0.16 \times VCI + 0.25 \times TCI + 0.48 \times TRCI + 0.11 \times DEM \quad (3)$$

In Eq. (1) to Eq. (3), CDI_{ij} represents the comprehensive drought index model in the i-th year and the j-th month, with a value ranging from 0 to 1 and a negative relationship between the magnitude of CDI and drought severity,PDI_{ij} is the PCA drought index model in the i-th year and the j-th month, with a value ranging from 0 to 1, and a negative relationship between the magnitude of PDI and drought severity, ADI is the optimal analytic hierarchy process drought index,w_1, w_2, w_3, and w_4 are the weight coefficients of VCI, TCI, TRCI, and elevation, respectively, and $w_1 + w_2 + w_3 + w_4 = 1$. More details on the construction of the model and the calculation of specific parameters can be found in the literature (Yu, 2020).

Within the verification of the CDI model, past studies have shown that CDI and SPI/SPEI are highly and significantly correlated at $P < 0.01$, and that there is a higher correlation between CDI and SPI. Moreover, there were relatively high correlation coefficients between the Kunming, Yuxi, and Yuanjiang stations in Central Yunnan Province, and CDI is better able to express meteorological drought (Yu, 2020). The drought grade was classified according to SPI, allowing the CDI drought grade to be obtained (Table 1). Finally, the evolutions in drought intensity, drought frequency, and drought change during the study period were analyzed.

3.2.2. Soil erosion model

Soil erosion in Central Yunnan Province was simulated using the RUSLE. The RUSLE is characterized by a simple structure, clear physical meaning of parameters, simple calculation, and strong practicability. The RUSLE expression is:

$$A = R \times K \times LS \times C \times P \quad (4)$$

In Eq. (4), A is the annual average soil erosion yield (t $hm^{-2}\cdot yr^{-1}$; after multiplying by 100, the unit is converted to t $km^{-2}\cdot yr^{-1}$); R is the rainfall erosivity factor (MJ·mm $hm^{-2}\cdot h^{-1}\cdot yr^{-1}$), K is the soil erodibility factor (t·h $MJ^{-1}\cdot mm^{-1}$), LS is the slope length and steepness factor, C is the vegetation cover management factor, and P is the soil and water conservation factor. More details on the calculation of the R, K, LS, C, and P factors can be found in the literature (Liu et al., 2020). The soil erosion in the Central Yunnan Province was categorized into six levels according to the SL190-2007 "soil erosion classification standard" issued by the Ministry of Water Resources of the People's Republic of China (Table 2).

By comparing the extent of soil erosion obtained by RUSLE with that determined by a report of soil erosion in Yunnan Province using remote sensing, Liu (2019) found that the proportion of soil erosion of Central Yunnan Province in 2000 was consistent with that of the remote sensing investigation in 1999 and that changes to the area of total erosion was consistent with the actual erosion situation.

3.2.3. Soil erosion intensity index (SEII)

A comprehensive index that can reflect the intensity of soil erosion is needed to compare and analyze the soil erosion in different spatial units of a catchment. The value of this index reflects the severity of soil erosion, which can be expressed by a SEII, which is calculated as:

$$SEII_j = 100 \times \sum_{i=1}^{6} w_i \times A_{ij}/S_j \quad (5)$$

In Eq. (5), $SEII_j$ is the soil erosion index of the j-th drought grade or county, and the value is positively related to the severity of soil erosion, w_i is the graded value of soil erosion intensity of grade i, A_{ij} is the soil erosion area of the j-th drought grade or county, and S_j is the area of the j-th drought grade or county. The grading values of micro, mild, moderate, strong, extremely strong, and severe soil erosion are 0, 2, 4, 6, 8, and 10 respectively, with the value having a positive relationship with the contribution to the soil erosion index.

4. Results

4.1. Analysis of drought change

Eq. (1) was used to calculate the comprehensive drought index (CDI) from November 2009 to April 2018, and pixels showing light drought were recorded as drought pixels. Drought coverage of Central Yunnan Province was calculated as the percentage of monthly drought in the total number of pixels (Fig. 2a). As shown in Fig. 2a, droughts occurred in all months except January 2015, November 2016, and April 2017, and were particularly prevalent in January 2010 and February 2011. The annual average drought coverage was obtained through aggregation of the monthly drought coverage. The percentage average drought coverage for multi-year dry-season droughts reached 42.81% before 2014 and decreased thereafter. The maximum percentage multi-year dry-season average drought coverage was in January at 64.10%, followed by February at 46.22%, with November experiencing the smallest drought coverage of 9.23%.

The average CDI of each month was calculated to obtain the average drought intensity of the dry season from 2010 to 2018 (Fig. 2b). Based on this measure, extreme and severe droughts over many years were mainly concentrated in the counties of Yuanmou, Yongren, Xinping, and Yuanjiang and in Kunming City, and the remaining areas mainly experienced light to moderate drought intensities. These results combined with the frequency of droughts shown in Fig. 2c indicated that areas experiencing high-intensity drought also showed higher frequencies of drought. The average dry season frequency of droughts during the 54 months from November 2009 to April 2018 was 18.33 months. There were mainly three regions in which droughts were experienced at a frequency exceeding 40, namely the counties of Yuanmou, Yongren, and Wuding in Chuxiong Prefecture, Shuangbai, Xinping, and Yuan-

Table 1
Categorization of the comprehensive drought index used in the current study.

Level	No drought	Light drought	Moderate drought	Heavy drought	Extremely drought
CDI	$0.36 < CDI$	$0.33 < CDI \leq 0.36$	$0.30 < CDI \leq 0.33$	$0.27 < CDI \leq 0.30$	$CDI \leq 0.27$

Table 2
Soil erosion classification standard according to the SL190-2007 "soil erosion classification standard" issued by the Ministry of Water Resources of the People's Republic of China.

Level	Average modulus of soil erosion (t/(km^2·a))	Average loss thickness (mm/a)
Micro	< 500	0.37
Mild	500–2,500	0.37–1.9
Moderate	2,500–5,000	1.9–3.7
Strong	5,000–8,000	3.7–5.9
Extremely strong	8,000–15,000	5.9–11.1
Severe	>15,000	>11.1

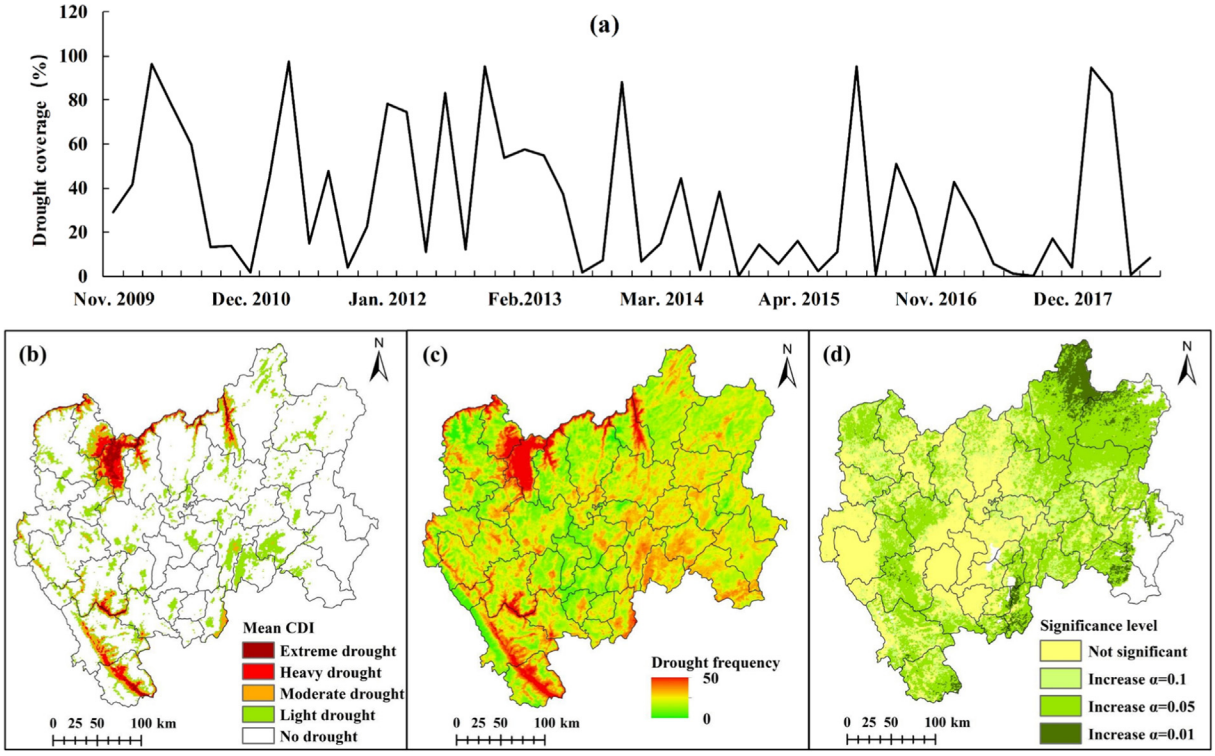

Fig. 2. Drought characteristics of Central Yunnan Province, China from 2009 to 2018. (a) Drought coverage of Central Yunnan Province during the dry season; (b) Mean value of the multi-year, dry-season comprehensive drought index (CDI); (c) Drought frequency (times); (d) Mann-Kendall (M−K) trend test of CDI during the dry season.

jiang in Yuxi City, and in Kunming City. The frequency of droughts in the central part of Central Yunnan Province was also relatively high, with most areas experiencing droughts at frequencies exceeding 20, whereas the cities of Jinning and Anning as well as Huize County experienced relatively low frequencies of droughts.

Fig. 2d shows the changes in dry season CDI in Central Yunnan Province over many years, as calculated through the Mann-Kendall (M−K) trend test. The results showed an increasing trend in CDI, whereas there was a weakening trend in drought. The proportion of total area in which CDI increased was 64.34% ($P < 0.1$), among which the proportions of total area in which there were significant ($P < 0.05$) and highly significant ($P < 0.01$) increasing trends in CDI were 39.30% and 5.07%, respectively, concentrated in the east and northeast.

4.2. Analysis of soil erosion

The average soil erosion values for Central Yunnan Province for 2010, 2015, 2018 obtained using the RUSLE were 1,769.54 t km^{-2}·yr^{-1}, 1,884.56 t km^{-2}·yr^{-1}, and 1,000.25 t km^{-2}·yr^{-1}, with a multi-year average of 1,551.45 t km^{-2}·yr^{-1}, thereby falling into the mild erosion category (Fig. 3a–c). There was an initial increase in soil erosion, with the maximum occurring in 2015, followed by a decrease, with most areas mainly experiencing micro and mild erosion. Extremely strong and severe erosion was mostly distributed in the mountains and river valleys in the north and southwest of Central Yunnan Province. The spatial distribution of soil erosion intensity showed a significant correlation with the topography of the region. As shown in Fig. 3d–f, the Soil Erosion Intensity Index

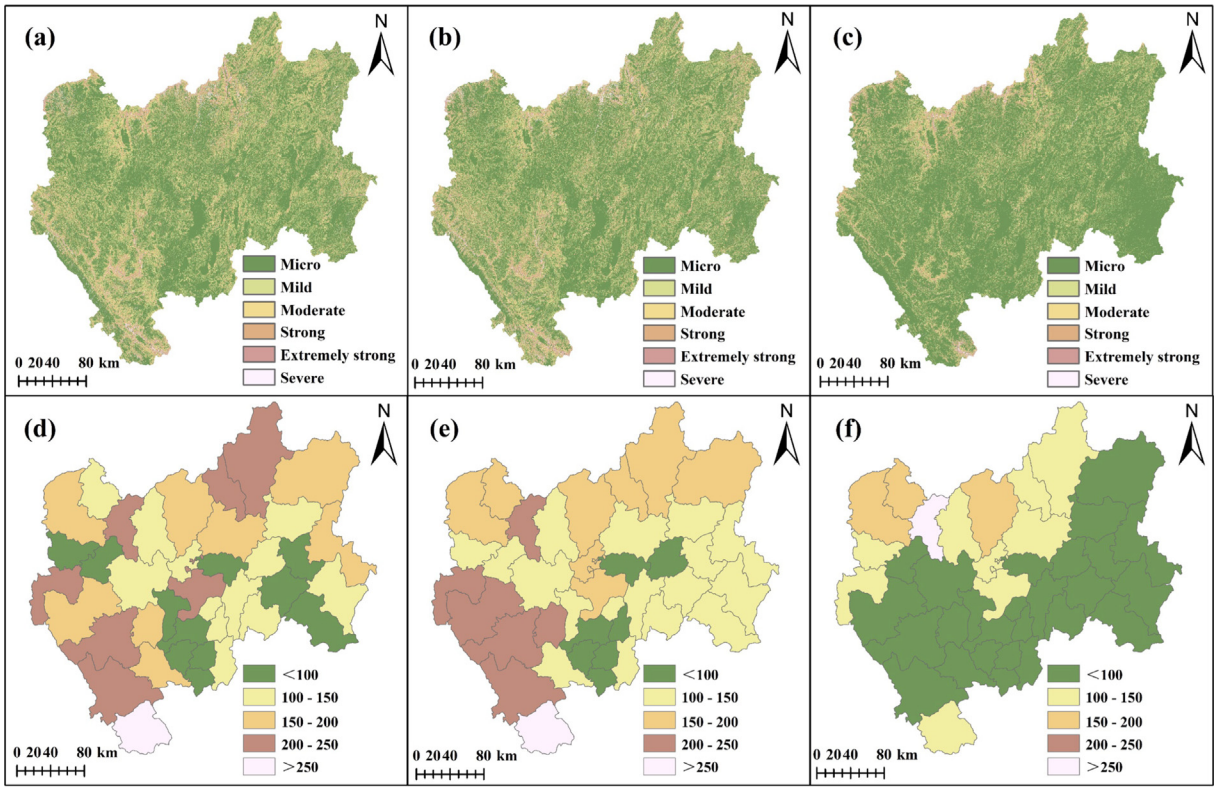

Fig. 3. Spatial distribution of soil erosion (a, b and c represent 2010, 2015, and 2018, respectively) and soil erosion intensity index (SEII) of each county (d, e, and f represent 2010, 2015, and 2018, respectively) within Central Yunnan Province, China from 2009 to 2018.

(SEII) analysis of soil erosion in various counties during 2010 indicated that SEII values of over two-thirds of the counties were 100. Among them, Yuanjiang County experienced the highest soil erosion, with an SEII value of 289.34. The SEII values of most counties by 2015 had increased compared with that of the previous period, with further increases in soil erosion. Soil erosion in the other counties decreased slightly by 2018, except in Yuanmou County in which SEII increased.

Calculation of the transfer in erosion grade between adjacent years (Table 3, Table 4) indicated that there was a decreasing trend in mild and moderate erosion in the area from 2010 to 2015. Although a net increasing trend in the area of micro erosion was maintained, the areas of strong, extremely strong, and severe erosion increased by 191.26 km^2, 316.19 km^2, and 194.36 km^2, respectively, and soil erosion showed a deteriorating trend. Overall, soil erosion decreased from 2015 to 2018, and although micro erosion showed an increasing trend, the remaining areas of intense erosion showed a net decrease in area. This indicated that soil erosion was effectively mitigated, and there was an overall improvement in the ecological environment of Central Yunnan Province.

4.3. Soil erosion under different drought grades

Soil erosion under different drought grades was analyzed using the SEII (Table 5). The results showed that the proportion of total area experiencing drought in 2010 reached 66.50% and that the largest value of SEII was that under the extreme drought grades. Although drought accounted for a relatively small proportion of total area

Table 3
Changes in soil erosion (km^2) of various grades in Central Yunnan Province, China from 2010 to 2015.

Level	2010	Soil erosion mutual transformation area from 2010 to 2015						Period decrease
		Micro	Mild	Moderate	Strong	Extremely strong	Severe	
Micro	56291.06	47512.93	5858.79	1618.06	639.66	356.65	304.97	8778.13
Mild	18112.15	7123.62	6901.98	2775.69	912.44	315.70	82.72	11210.17
Moderate	10347.84	1965.82	2887.48	3266.62	1603.18	522.31	102.44	7081.23
Strong	5267.43	595.99	795.13	1340.14	1524.64	883.10	128.43	3742.79
Extremely strong	3176.64	354.46	229.67	397.84	698.36	1155.63	340.68	2021.01
Severe	1362.88	325.56	43.59	55.88	80.42	259.43	598.01	764.87
Period increase		10365.45	9814.65	6187.61	3934.06	2337.20	959.23	
Increase - decreases		1587.32	−1395.52	−893.62	191.26	316.19	194.36	

Table 4
Changes in soil erosion (km^2) of various grades in Central Yunnan Province, China from 2015 to 2018.

Level	2015	Soil erosion mutual transformation area from 2015 to 2018						Period decrease
		Micro	Mild	Moderate	Strong	Extremely strong	Severe	
Micro	57878.67	53382.07	3040.09	939.03	346.68	147.88	22.92	4496.59
Mild	16716.65	9539.22	5349.64	1361.29	354.00	101.79	10.70	11367.01
Moderate	9454.21	3691.37	2585.07	2214.93	750.06	195.50	17.27	7239.28
Strong	5458.70	1573.51	996.35	1497.03	1000.92	364.54	26.35	4457.79
Extremely strong	3492.82	872.96	378.54	609.35	793.64	735.03	103.30	2757.79
Severe	1556.95	645.75	115.26	129.07	139.27	289.12	238.48	1318.48
Period increase		16322.82	7115.30	4535.78	2383.65	1098.84	180.54	
Increase - decreases		11826.23	−4251.71	−2703.50	−2074.14	−1658.95	−1137.93	

Table 5
The percentage of soil erosion (%) and soil erosion index under different drought levels within Central Yunnan Province, China from 2010 to 2018.

Year	Drought Level	drought/%	Micro	Mild	Moderate	Strong	Extremely strong	Severe	SEII
2010	No drought	33.50	69.79	15.81	7.60	3.46	1.87	1.03	108.06
	Light drought	27.96	57.89	21.38	11.40	5.38	2.59	0.96	150.92
	Moderate drought	15.22	51.82	23.81	13.51	6.56	3.25	0.91	176.11
	Heavy drought	15.93	46.48	25.85	14.41	7.85	4.21	1.10	201.12
	Extremely drought	7.39	34.73	21.91	17.63	12.18	9.80	3.21	297.93
2015	No drought	94.71	61.14	18.47	10.10	5.45	3.08	1.26	147.30
	Light drought	4.69	29.00	22.15	18.61	13.99	11.26	3.72	330.01
	Moderate drought	0.50	22.39	16.96	14.78	17.17	16.96	9.13	423.04
	Heavy drought	0.10	21.43	19.39	15.31	15.31	16.33	11.22	434.69
	Extremely drought	0.00	0.00	0.00	0.00	0.00	0.00	0.00	0.00
2018	No drought	89.25	76.54	12.41	6.20	2.77	1.23	0.23	78.40
	Light drought	5.11	50.76	20.18	14.42	8.31	4.83	0.86	195.19
	Moderate drought	2.66	38.83	21.36	15.97	11.92	8.55	1.99	266.40
	Heavy drought	1.65	29.76	20.40	17.09	14.10	10.53	4.48	322.81
	Extremely drought	1.33	24.11	18.69	19.09	14.40	12.06	4.05	337.06

in 2015, and there were no incidents of extreme drought, SEII showed an increasing trend with increased drought grade, and the SEII value in 2015 exceeded that under the same drought grade in 2010. Similarly, the change in SEII in 2018 was consistent with those during the two previous periods. Overall, the drought intensity showed positive relationships with the SEII and soil erosion.

5. Discussion

5.1. Drought characteristics and models

According to Chen (2018, 2020); Zhao and Huang (2012); Zhao and Huang (2014); Zhao and Huang (2016), Kunming City, Chuxiong Prefecture, Yuxi City, and Qujing City suffered continuous droughts in autumn, winter, and spring during 2010. These droughts were of long duration and wide spatial coverage and represented the most serious drought disasters since meteorological records began. Kunming City and the Yuxi, and Chuxiong prefectures experienced droughts for five consecutive years from 2009 to 2014, during which precipitation and temperature were lower and higher than that in previous years, respectively. The El Niño event from 2014 to 2016 resulted in a relatively severe early summer high temperature and drought in 2015. However, Central Yunnan Province received above average rainfall 2015, characterized by isolated rainstorms, frequent flood disasters, and low incidence of drought. Conditions in 2017 included greater rainfall, lower temperature, and lower average sunshine hours than that in previous years, resulting in mainly low levels of drought. No precipitation occurred in most parts of Yunnan Province in January 2018, whereas precipitation during February 2018 decreased by 50%, resulting in a more serious drought. Above average precipitation in March effectively alleviated the development of drought in most areas (http://www.weather.com.cn/). In addition, Yu (2020) indicated that the percentage drought coverage in Yunnan Province during 2009–2014 exceeded that during 2015–2018, and with high frequency droughts occurring in Chuxiong Prefecture, Kunming City, and Yuxi City, consistent with the drought characteristics in Fig. 2 of the present study.

A comprehensive drought index that considers multiple factors is better able to capture the complex process and various effects of drought compared with a single drought index (Jiao et al., 2019). Principle component analysis (PCA) can effectively integrate multiple correlation variables into a few variables, which not only reduces the difficulty of analyzing the problem, but also minimizes the loss of valuable information in the variables, thereby ensuring the accuracy of the analysis results (Pearson, 1901).

Therefore, PCA is widely used in drought research (Arun Kumar et al., 2021; Kim et al., 2021). The current study used factor analysis to effectively compress and reduce the dimension of the datasets of the four indicators [tropical rainfall condition index (TRCI), vegetation condition index (VCI), temperature condition index (TCI), elevation]. PCA was conducted to obtain the weight coefficient of each index month (normalized weight coefficient), following which the PCA drought index (PDI) model was obtained. The temperature vegetation drought index (TVDI) has been more widely used in the drought model compared to in more extensive and more mature drought models (Chen et al., 2017; Hou and Zhang, 2017), with TVDI used within verification by PCA and analytic hierarchy process (AHP). There was a relatively high correlation between PDI and TVDI. For example, the correlation coefficient between PDI and TVDI in January 2018 was −0.785 ($P < 0.01$) (Table 6). Therefore PDI was better able to express the agricultural drought situation (Kulkarni et al., 2020). Although PCA can completely rely on the objective information of the sample, using PCA to obtain a reflection of the actual situation is difficult as it ignores subjective value judgments.

AHP is a mathematical quantification based on the empirical knowledge of the decision maker and assesses the relative importance of each level of elements, following which each sample is evaluated and ranked (Wei et al., 2020). The 5-level scaling method was used in AHP to construct the assessment matrix (Yu, 2020). The correlation coefficients between the four indicators (TRCI, VCI, TCI, and elevation) and standardized precipitation index / standardized precipitation evapotranspiration index (SPI / SPEI) were used as references of the relative importance of each indicator, and the relative importance of each indicator was determined by combining the research experience and the characteristics of each indicator (Du et al., 2013; Wang et al., 2018). The final constructed optimal analytic hierarchy process drought index (ADI) showed a good correlation with TVDI. For example, there was a significant correlation between ADI and TVDI in January 2018 with a correlation coefficient of − 0.394 ($P < 0.01$) (Table 6). Although AHP can reasonably add prior knowledge into the evaluation process, it ignores the interrelationships between the indicators reflected by the objective data of the sample, and the error in subjective knowledge will also have a greater impact on the accuracy of the results (Kim et al., 2021).

Table 6
Correlation coefficients between temperature vegetation drought index (TVDI) and three drought models (January 2018) for Central Yunnan Province, China.

Drought model	PDI	ADI	CDI
R	−0.785**	−0.394**	−0.810**

Note: ** indicating significance at $P < 0.01$

The results of the CDI model showed a significant ($P < 0.01$) correlation with SPI/SPEI. The correlation coefficient between CDI and TVDI exceeded those between PDI and TVDI, ADI and TVDI (Table 6). In addition, past studies have shown that drought monitoring using the CDI provides results that are more consistent with actual drought conditions compared to those of other drought indices (Ji et al., 2018; Yu, 2020). Therefore, the present study constructed a more realistic CDI by combining the objectivity of the PCA with the subjectivity of the AHP. In general, the use of the CDI in drought monitoring has been more successful in reflecting agricultural and meteorological droughts as compared to the use of single drought indices such as the PDI and ADI (Yu, 2020).

5.2. Soil erosion factors and verification

Although a more realistic simulation of soil erosion was obtained through the Revised Universal Soil Loss Equation (RUSLE) with consideration of important factors affecting erosion such as precipitation, soil, topography, vegetation coverage, and water and soil conservation measures, the spatial distribution of some erosion factors was uneven. As shown in Fig. 4a, the value of the rainfall erosivity (R) factor was low in the northeast corner of Central Yunnan Province and high in the southeast, southwest, and northwest corners. However, the R factor in Qujing City increased from northwest to southeast, which could be attributed to the large area of the city, the overall topography showing an inclination from northwest to southeast, and the distribution of the river system in the southeast being more developed than that in the northwest. However, Kunming and Yuxi appeared to be affected by the Dianchi, Fuxian, and Qilu lakes, resulting in relatively small differences in rainfall and consequently relatively uniform R scores. As shown in Fig. 4b, the maximum values of the soil erodibility (K) factor in the counties of Huize, Xinping, and Eshan showed a patchy distribution. This result could be attributed to the maximum area of the K factor in Huize County being dominated by yellow brown soil, whereas the counties of Xinping and Eshan are dominated by red soil. This result shows that the spatial distribution of the maximum value of the K factor had a weak correlation with soil types, and the soil texture and organic carbon content in the region may play a dominant role in soil erosion. The K factor is also closely related to climate change. For example, soil erodibility is exacerbated by decreased precipitation, increased evapotranspiration, and more prolonged dry periods, resulting in some areas being more susceptible to erosion (Baskan, 2021). Furthermore, hydrophobicity drastically reduces the affinity of soil for water after prolonged drought periods (Gimbel et al., 2016). Therefore, obtaining more realistic future predictions of soil erosion requires the consideration of the effects of drought,

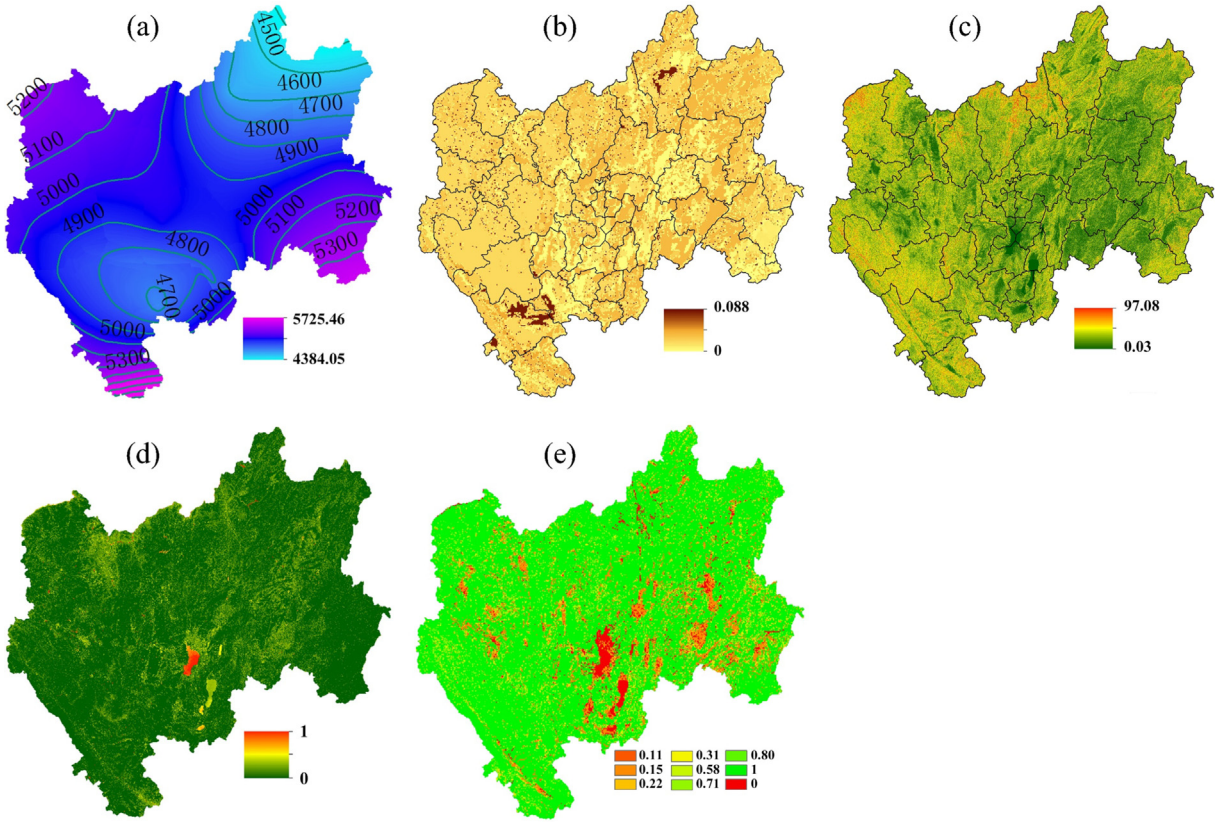

Fig. 4. The spatial distributions of the different factors within the Revised Universal Soil Loss Equation (RUSLE) for Central Yunnan Province, China for 2018. (a) rainfall erosivity (R) factor; (b) soil erodibility (K) factor; (c) slope length and steepness (LS) factor; (d) vegetation cover management (C) factor; (e) soil and water conservation (P) factor.

which can be achieved mainly through improving the K factor in hydrological models.

Past studies have found that slope length affects soil erosion (Tsegaye and Bharti, 2021). As shown in Fig. 4c, the spatial distribution of the slope length and steepness (LS) factor in Central Yunnan Province is basically consistent with the overall topography. An increase in the LS factor corresponded with heightened erosion due to increased velocity of water flow (Haan et al., 1994; Piyathilake et al., 2021). The present study used the approach of Liu et al. (2000) to estimate the LS factor for the RUSLE. McCool et al. (1987) provided a methodology for estimating LS with a broader field of applicability, thereby allowing the estimation of soil erosion from various terrains (e.g. rangelands, forests, disturbed sites, and steep slopes). The use of this approach has shown good performance in estimating soil erosion (Efthimiou et al., 2020).

The dimensionless vegetation cover management (C) factor is an important erosion factor reflecting the influence of different vegetation coverage on soil erosion (Phinzi and Ngetar, 2019). The value of the C factor is inversely proportional to degree of local vegetation coverage since denser vegetation strongly protects against soil erosion (Efthimiou et al., 2020). Besides for lakes, the results of the current study showed that areas with higher C values were prone to soil erosion (Fig. 4d).

The dimensionless soil and water conservation (P) factor is one of the most difficult factors to determine (Tian et al., 2021) and represents the ratio of the amount of soil loss over a certain period time, with a value ranging from 0 to 1 (Peng et al., 2018). As shown in Fig. 4e, most areas had high P values ranging from 0.8 to 1, indicating that most parts of Central Yunnan Province are prone to soil erosion. The determination of the P value in the RUSLE mainly depended on land use types (Behera et al., 2020). The high accuracy of the land cover classification in Central Yunnan Province of 72.24% allowed the P factors for Central Yunnan Province to be calculated (Liu, 2019).

In addition, the factor detector in the geographic detector was used to explore the correlation and difference between the four natural factors of vegetation coverage, slope, elevation, and annual precipitation (Wang et al., 2010), as well as the spatial distribution of soil erosion from 2010 to 2018 (Table 7). The q value was used to evaluate the degree of influence, with its value ranging from 0 to 1 (Wang et al., 2010), and with positive relationships with the significance of the spatial divergence of soil erosion and the degree of influence of natural factors. As shown in Table 7, vegetation coverage factors played a leading role in the influence of the distribution of soil erosion intensity, with q values exceeding 0.28, and the intensity of soil erosion in high vegetation coverage areas being relatively

Table 7
The influence of natural factors on soil erosion intensity within Central Yunnan Province, China from 2009 to 2018.

Region	Year	Vegetation coverage	Slope	Elevation	Annual precipitation
Kunming	2010	0.30	0.13	0.01	0.01
	2015	0.29	0.09	0.01	0.02
	2018	0.28	0.07	0.02	0.03
Yuxi	2010	0.36	0.11	0.09	0.01
	2015	0.36	0.08	0.04	0.02
	2018	0.32	0.03	0.05	0.06
Qujing	2010	0.28	0.11	0.00	0.01
	2015	0.30	0.06	0.00	0.02
	2018	0.29	0.03	0.00	0.05
Chuxiong	2010	0.40	0.08	0.05	0.00
	2015	0.41	0.07	0.04	0.01
	2018	0.41	0.05	0.03	0.00

low. Therefore, the reduction in soil erosion through vegetation restoration is extremely important for sustainable development. The degree of influence of slope on soil erosion was slightly smaller than that of vegetation coverage, with a maximum q value of 0.13. Slope affected the speed of water flow and the direction and quantity of surface runoff. Therefore, there was a positive relationship between slope steepness and the affect by surface runoff (Olorunfemi et al., 2020). The influence of altitude and annual rainfall was small (Table 7).

The simulations of soil erosion obtained in the current study were compared to those obtained by Ding et al. (2018) using the Chinese Soil Loss Equation (CSLE) to estimate the land erosion status of Yunnan Province in 2015 (Table 8 and Table 9). The results showed that the two methods obtained similar areas of total soil erosion and area proportions of each erosion intensity grade, indicating that the RUSLE model performed well in estimating the soil erosion status of Central Yunnan Province when compared with the CSLE model, consistent with the conclusions obtained by Peng et al. (2018). In addition, past studies have shown that the RUSLE provides an efficient method of estimating soil erosion in complex areas with irregular precipitation and ecological fragility (da Cunha et al., 2017; Li et al., 2020; Peng et al., 2018).

The average soil erosion from 2010 to 2018 showed a general trend of first increasing to 1,884.56 t $km^{-2}{\cdot}yr^{-1}$ and then decreasing to 1,000.25 t $km^{-2}{\cdot}yr^{-1}$ (Fig. 3). Both the modulus and area of soil erosion reached their ten-year minimums in 2018 (Liu et al., 2020). This result could be attributed to the gradual improvement in various types of infrastructure in Central Yunnan Province as well as an increasing awareness of environmental protection among the population. Sustainable development in the Central Yunnan Province has been promoted though water and soil conservation measures and effective reductions in activities that are damaging to the ecology, resulting in reductions in soil erosion and clear advancements in drought resistance and disaster reduction.

Table 8
Comparisons of areas of Central Yunnan Province experiencing different categories of soil erosion in 2015 as a proportion (%) of total area as simulated in the study by Ding et al. (2018) and in the current study.

Comparison	Micro erosion	Total soil erosion
Ding et al. (2018)	67.88	32.12
In our study	61.21	38.79

5.3. Changes in drought characteristics under different soil erosion grades

The process of soil erosion results in destruction of vegetation and soil structure (Xu et al., 2016), and the imbalance between precipitation and surface water/groundwater results in water shortages and hydrological drought (Shi, 1996). The imbalance between soil water and crop water demand results in water shortages and agricultural droughts (Shi, 1996). The destruction of forest vegetation decreases its unique function of regulating surface temperature and air humidity (Pickering et al., 2021). The soil temperature of a barren slope and the temperature of the near soil layer increases under the scorching sun, resulting in excessive evaporates rates, which can easily lead to drought (Blanken, 2014). Moreover, the loss of water, soil, and fertilizer results in poor water conservation capacity of sloping farmland, which also aggravates the occurrence of drought. The destruction of the soil layer decreases the water storage capacity of the vegetation and the soil system in areas experiencing high soil erosion (Magesh and Chandrasekar, 2016). In addition, soils under drought conditions are prone to hydrophobicity (Gazol et al., 2018; Gimbel et al., 2016), thereby hindering the infiltration of surface water after rainfall and intensifying surface runoff and soil erosion (Ahn et al., 2013; Zhao et al., 2011).

The multi-year average soil erosion across 2010, 2015, and 2018 and the changes in multi-year dry-season drought characteristics under each erosion grade and the correlation coefficient between soil erosion and drought characteristics were calculated (Table 10). The frequency of drought increased with increasing soil erosion intensity from 17.00 to 30.20. The correlation coefficient between soil erosion intensity and dry-season drought frequency was 0.2623,

Table 9
Comparisons of areas of Central Yunnan Province experiencing different categories of soil erosion over many years as a proportion (%) of total area as simulated in the study by Ding et al. (2018) and in the current study.

Comparison	Mild	Moderate	Strong	Extremely strong	Severe
Ding et al. (2018)	64.39	17.00	9.28	6.46	2.87
In our study	45.58	25.78	14.88	9.52	4.24

Table 10
Relationship between droughts and soil erosion within Central Yunnan Province between 2009 and 2018.

Grades	Erosion area (km^2)	% of area	Mean drought frequency	Mean CDI
Micro	71,560,878	68.99271	17.00	0.40
Mild	18,841,033	18.16487	20.02	0.39
Moderate	8,299,306	8.001462	22.35	0.37
Strong	3,710,674	3.577506	24.27	0.36
Extremely strong	1,152,362	1.111006	28.27	0.34
Severe	158,121	0.152446	30.20	0.33
Drought characteristics	drought frequency	Mean CDI		
R	0.2623	−0.2679		

Abbreviations: CDI: comprehensive drought index.

whereas that between soil erosion intensity and drought intensity was − 0.2679, indicating a positive relationship between the intensity of soil erosion and the frequency and intensity of drought. Consistent with the results of the present study, Santra and Santra Mitra (2020) obtained correlation coefficients between soil erosion and drought frequency and between soil erosion and the average annual drought monitoring index of 0.2049 and 0.2719, respectively, indicating that the increase in soil erosion was closely related to the frequency and intensity of drought.

Conversely, as shown in Table 5, drought may also increase soil erosion. Soil water content is reduced during drought disasters, and soil moisture is insufficient to maintain the needs of vegetation growth, resulting in the death and decomposition of vegetation and crops (Yang et al., 2018). During subsequent floods, excessive groundwater levels result in soil saturation, leading to the inhibition or even death of crop roots (Hubbard and Wu, 2005). Since the soil has lost the binding action of vegetation roots due to the preceding drought, heavy rainfall events result in increased mobilization of soil, leading in increased soil erosion intensity.

Soil erosion in Central Yunnan Province increased the frequency of flood and drought disasters, which further weakened the functioning of ecosystem soil conservation services, thereby intensifying the intensity and speed of soil erosion and forming a positive feedback mechanism. The improvements in soil and water conservation measures in Central Yunnan Province have resulted in the gradual improvement in the ecological environment, an increased water storage capacity of the land, and decreases in soil erosion and drought (Liu et al., 2020). Therefore, effective mitigation of floods and droughts requires sustainable ecological development as well as water and soil conservation measures.

6. Conclusions

The current study focused on the Central Yunnan Province as the economic hub of Yunnan Province. PCA and AHP were applied to determine the weight coefficients of each drought index based on MODIS, TRMM, and DEM data. The CDI was then constructed and used to explore the dynamics of drought during the dry season over the past decade. The RUSLE was used to quantitatively characterize the soil erosion status of Central Yunnan Province from 2010 to 2018. Finally, the SEII was used to analyse the soil erosion status of each county under different drought grades. The present study came to the following conclusions:

(1) The CDI constructed by considering multiple drought factors and combining subjective and objective methods was a reliable indicator for drought assessment. The average drought coverage percentage and average drought frequency of the Central Yunnan Province were 33.98% and 18.33 times, respectively. Although there was a higher drought frequency in areas with high drought intensity, dry season drought showed a weakening trend for many years, which was most significant in the northeast Central Yunnan Province.
(2) Soil erosion generally showed a trend of first increasing and then decreasing. Soil erosion intensities were mainly micro, mild, and moderate, and soil erosion showed an improving trend. The vegetation coverage factor and slope had a greater influence on the distribution of soil erosion intensity, and dynamic monitoring of these two factors could be used to identify the general trend in the spatial distribution of soil erosion.

(3) SEII was shown to be a good indicator of the severity of soil erosion in each county. High values of SEII were mainly concentrated in the southwestern and northern parts of Central Yunnan Province, and SEII showed a trend of first increasing and then decreasing in most counties from 2010 to 2018. In addition, SEII could be used to characterize soil erosion in areas with different drought grades. The SEII value increased with the increasing drought grades.

Central Yunnan Province tends to be a focal point of the frequent natural disasters in Yunnan Province. Therefore, the relevant regulatory agencies should strive to improve natural disaster prevention and mitigation measures in Central Yunnan Province. Some proposed measures include: (1) Monitoring of natural disasters, with particular attention on the dynamics and evolution of drought and flood. (2) A strengthening of natural disaster emergency response capabilities. (3) An increased focus on heightening public awareness of natural disaster prevention and mitigation.

Declaration of Competing Interest

The authors declare that they have no known competing financial interests or personal relationships that could have appeared to influence the work reported in this paper.

Acknowledgements

The authors are very grateful to the anonymous reviewers and editors for their thoughtful review comments and suggestions which have significantly improved this paper. This research was funded by the Multi-government International Science and Technology Innovation Cooperation Key Project of National Key Research and Development Program of China for "Environmental monitoring and assessment of land use/land cover change impact on ecological security using geospatial technologies", grant number 2018YFE0184300; by the Key Program of Basic Research of Yunnan Province of China for the "Scientific Investigation on the Geographical Environment of the Tourism Health Industry in the Tropic of Cancer (Yunnan Section)", grant number 2019FA017; and by the Program for Innovative Research Team (in Science and Technology) at the University of Yunnan Province, IRTSTYN.

References

Ahn, S., Doerr, S.H., Douglas, P., Bryant, R., Hamlett, C.A.E., McHale, G., Newton, M.I., Shirtcliffe, N.J., 2013. Effects of hydrophobicity on splash erosion of model soil particles by a single water drop impact. Earth Surface Processes and Landforms 38 (11), 1225–1233. https://doi.org/10.1002/esp.3364.

Almohamad, H., 2020. Impact of Land Cover Change Due to Armed Conflicts on Soil Erosion in the Basin of the Northern Al-Kabeer River in Syria Using the RUSLE Model. Water 12 (12), 3323. https://doi.org/10.3390/w12123323.

Arun Kumar, K.C., Reddy, G.P.O., Masilamani, P., Turkar, S.Y., Sandeep, P., 2021. Integrated drought monitoring index: A tool to monitor agricultural drought by using time-series datasets of space-based earth observation satellites. Advances in Space Research 67 (1), 298–315. https://doi.org/10.1016/j.asr.2020.10.003.

Balti, H., Ben Abbes, A., Mellouli, N., Farah, I.R., Sang, Y., Lamolle, M., 2020. A review of drought monitoring with big data: Issues, methods, challenges and research directions. Ecological Informatics 60. https://doi.org/10.1016/j.ecoinf.2020.101136 101136.

Baskan, O., 2021. Analysis of spatial and temporal changes of RUSLE-K soil erodibility factor in semi-arid areas in two different periods by conditional simulation. Archives of Agronomy and Soil Science 1–13. https://doi.org/10.1080/03650340.2021.1922673.

Behera, M., Sena, D.R., Mandal, U., Kashyap, P.S., Dash, S.S., 2020. Integrated GIS-based RUSLE approach for quantification of potential soil erosion under future climate change scenarios. Environmental Monitoring and Assessment 192 (11), 733. https://doi.org/10.1007/s10661-020-08688-2.

Bento, V.A., Gouveia, C.M., DaCamara, C.C., Trigo, I.F., 2018. A climatological assessment of drought impact on vegetation health index. Agricultural and Forest Meteorology 259, 286–295. https://doi.org/10.1016/j.agrformet.2018.05.014.

Bircher, P., Liniger, H.P., Prasuhn, V., 2019. Comparing different multiple flow algorithms to calculate RUSLE factors of slope length (L) and slope steepness (S) in Switzerland. Geomorphology 346. https://doi.org/10.1016/j.geomorph.2019.106850 106850.

Blanken, P.D., 2014. The effect of winter drought on evaporation from a high-elevation wetland. Journal of Geophysical Research: Biogeosciences 119 (7), 1354–1369. https://doi.org/10.1002/2014JG002648.

Chen, C.F., Son, N.T., Chen, C.R., Chiang, S.H., Chang, L.Y., Valdez, M., 2017. Drought monitoring in cultivated areas of Central America using multi-temporal MODIS data. Geomatics, Natural Hazards and Risk 8 (2), 402–417. https://doi.org/10.1080/19475705.2016.1222313.

Chen, Q., 2018. Yunnan Jianzai Nianjian (2016–2017). Yunnan Science and Technology Press, Kunming.

Chen, Q., 2020. Yunnan Jianzai Nianjian (2018). Yunnan Science and Technology Press, Kunming.

Ciampalini, R., Constantine, J.A., Walker-Springett, K.J., Hales, T.C., Ormerod, S.J., Hall, I.R., 2020. Modelling soil erosion responses to climate change in three catchments of Great Britain. Science of The Total Environment 749. https://doi.org/10.1016/j.scitotenv.2020.141657 141657.

da Cunha, E.R., Bacani, V.M., Panachuki, E., 2017. Modeling soil erosion using RUSLE and GIS in a watershed occupied by rural settlement in the Brazilian Cerrado. Natural Hazards 85 (2), 851–868. https://doi.org/10.1007/s11069-016-2607-3.

Ding, J., Chen, Q., Tao, Y., Li, J., 2018. Dynamic Change and Spatial Characteristics of Soil Erosion in Yunnan Province. Journal of West China Forestry Science 047 (006), 15–21.

Ding, X., Dai, T., Bao, C., Pu, Z., 2011. Geological hazards preventing zoning in central area of Yunnan Province. The Chinese Journal of Geological Hazard and Control 22 (02), 69–75.

Du, L., Tian, Q., Yu, T., Meng, Q., Jancso, T., Udvardy, P., Huang, Y., 2013. A comprehensive drought monitoring method integrating MODIS and TRMM data. International Journal of Applied Earth Observation and Geoinformation 23, 245–253. https://doi.org/10.1016/j.jag.2012.09.010.

Efthimiou, N., Lykoudi, E., Psomiadis, E., 2020. Inherent relationship of the USLE, RUSLE topographic factor algorithms and its impact on soil erosion modelling. Hydrological Sciences Journal 65 (11), 1879–1893. https://doi.org/10.1080/02626667.2020.1784423.

Gao, J., Wang, H., 2019. Temporal analysis on quantitative attribution of karst soil erosion: A case study of a peak-cluster depression basin in Southwest China. CATENA 172, 369–377. https://doi.org/10.1016/j.catena.2018.08.035.

Gazol, A., Camarero, J.J., Jiménez, J.J., Moret-Fernández, D., López, M. V., Sangüesa-Barreda, G., Igual, J.M., 2018. Beneath the canopy: Linking drought-induced forest die off and changes in soil properties.

Forest Ecology and Management 422, 294–302. https://doi.org/10.1016/j.foreco.2018.04.028.

Gharibreza, M., Bahrami Samani, A., Arabkhedri, M., Zaman, M., Porto, P., Kamali, K., Sobh-Zahedi, S., 2021. Investigation of on-site implications of tea plantations on soil erosion in Iran using 137Cs method and RUSLE. Environmental Earth Sciences 80 (1), 34. https://doi.org/10.1007/s12665-020-09347-y.

Gimbel, K.F., Puhlmann, H., Weiler, M., 2016. Does drought alter hydrological functions in forest soils? Hydrol. Earth Syst. Sci. 20 (3), 1301–1317. https://doi.org/10.5194/hess-20-1301-2016.

Haan, C.T., Barfield, B.J., Hayes, J.C., 1994. Front Matter. In: Haan, C. T., Barfield, B.J., Hayes, J.C. (Eds.), Design Hydrology and Sedimentology for Small Catchments. Academic Press, San Diego, p. iii.

Han, L., Zhang, Q., Ma, P., Jia, J., Wang, J., 2016. The spatial distribution characteristics of a comprehensive drought risk index in southwestern China and underlying causes. Theoretical and Applied Climatology 124 (3), 517–528. https://doi.org/10.1007/s00704-015-1432-z.

Hou, L.Q., Zhang, J., 2017. Spatiotemporal Variation of Surface Soil Moisture Based on Temperature Vegetation Dryness Index (TVDI) in Qinshui Coalfield. Research of Soil and Water Conservation 3, 032.

Huang, D., Yang, X., Cai, H., Xiao, Z., Han, D., 2019. Identifying Human-Induced Spatial Differences of Soil Erosion Change in a Hilly Red Soil Region of Southern China. Sustainability 11 (11), 3103.

Hubbard, K.G., Wu, H., 2005. Modification of a Crop-Specific Drought Index for Simulating Corn Yield in Wet Years. Agronomy Journal 97 (6), 1478–1484. https://doi.org/10.2134/agronj2004.0227.

Javed, T., Yao, N., Chen, X., Suon, S., Li, Y., 2020. Drought evolution indicated by meteorological and remote-sensing drought indices under different land cover types in China. Environmental Science and Pollution Research 27 (4), 4258–4274. https://doi.org/10.1007/s11356-019-06629-2.

Jehanzaib, M., Sattar, M.N., Lee, J.-H., Kim, T.-W., 2020. Investigating effect of climate change on drought propagation from meteorological to hydrological drought using multi-model ensemble projections. Stochastic Environmental Research and Risk Assessment 34 (1), 7–21. https://doi.org/10.1007/s00477-019-01760-5.

Ji, T., Li, G., Yang, H., Liu, R., He, T., 2018. Comprehensive drought index as an indicator for use in drought monitoring integrating multi-source remote sensing data: a case study covering the Sichuan-Chongqing region. International Journal of Remote Sensing 39 (3), 786–809. https://doi.org/10.1080/01431161.2017.1392635.

Jia, L., Lu, J., 2012. Ecological factors of drought: A case study in Yunnan Province. Water Resources Protection 28(02), 54-56+81.

Jiao, W., Tian, C., Chang, Q., Novick, K.A., Wang, L., 2019. A new multi-sensor integrated index for drought monitoring. Agricultural and Forest Meteorology 268, 74–85. https://doi.org/10.1016/j.agrformet.2019.01.008.

Jin, F., Yang, W., Fu, J., Li, Z., 2021. Effects of vegetation and climate on the changes of soil erosion in the Loess Plateau of China. Science of The Total Environment 773. https://doi.org/10.1016/j.scitotenv.2021.145514 145514.

Kebede, Y.S., Endalamaw, N.T., Sinshaw, B.G., Atinkut, H.B., 2021. Modeling soil erosion using RUSLE and GIS at watershed level in the upper beles. Ethiopia. Environmental Challenges 2. https://doi.org/10.1016/j.envc.2020.100009 100009.

Kim, J.E., Yu, J., Ryu, J.H., Lee, J.H., Kim, T.W., 2021. Assessment of regional drought vulnerability and risk using principal component analysis and a Gaussian mixture model. Natural Hazards. https://doi.org/10.1007/s11069-021-04854-y.

KOGAN, F.N., 1990. Remote sensing of weather impacts on vegetation in non-homogeneous areas. International Journal of Remote Sensing 11 (8), 1405–1419. https://doi.org/10.1080/01431169008955102.

Kogan, F.N., 1995. Application of vegetation index and brightness temperature for drought detection. Advances in space research 15 (11), 91–100. https://doi.org/10.1016/0273-1177(95)00079-T.

Konapala, G., Mishra, A.K., Wada, Y., Mann, M.E., 2020. Climate change will affect global water availability through compounding changes in seasonal precipitation and evaporation. Nature Communications 11 (1), 3044. https://doi.org/10.1038/s41467-020-16757-w.

Kourgialas, N.N., 2020. Hydroclimatic impact on mediterranean tree crops area – Mapping hydrological extremes (drought/flood) prone parcels. Journal of Hydrology 596, 125684. https://doi.org/10.1016/j.jhydrol.2020.125684.

Kulkarni, S.S., Wardlow, B.D., Bayissa, Y.A., Tadesse, T., Svoboda, M. D., Gedam, S.S., 2020. Developing a Remote Sensing-Based Combined Drought Indicator Approach for Agricultural Drought Monitoring over Marathwada, India. Remote Sensing 12 (13), 2091. https://doi.org/10.3390/rs12132091.

Lee, S., Chu, M.L., Guzman, J.A., Botero-Acosta, A., 2020. A comprehensive modeling framework to evaluate soil erosion by water and tillage. Journal of Environmental Management 279. https://doi.org/10.1016/j.jenvman.2020.111631 111631.

Li, H., Zhu, H., Wei, X., Liu, B., Shao, M., 2021. Soil erosion leads to degradation of hydraulic properties in the agricultural region of Northeast China. Agriculture, Ecosystems & Environment 314. https://doi.org/10.1016/j.agee.2021.107388 107388.

Li, J., Sun, R., Xiong, M., Yang, G., 2020. Estimation of soil erosion based on the RUSLE model in China. Acta Ecologica Sinica 40 (10), 3473–3485.

Li, S., Lobb, D.A., Kachanoski, R.G., McConkey, B.G., 2011. Comparing the use of the traditional and repeated-sampling-approach of the 137Cs technique in soil erosion estimation. Geoderma 160 (3), 324–335. https://doi.org/10.1016/j.geoderma.2010.09.029.

Li, Y., Qi, S., Liang, B., Ma, J., Cheng, B., Ma, C., Qiu, Y., Chen, Q., 2019. Dangerous degree forecast of soil loss on highway slopes in mountainous areas of the Yunnan-Guizhou Plateau (China) using the Revised Universal Soil Loss Equation. Natural Hazards Earth System Sciences 19 (4), 757–774. https://doi.org/10.5194/nhess-19-757-2019.

Liu, B.Y., Nearing, M.A., Shi, P.J., Jia, Z.W., 2000. Slope Length Effects on Soil Loss for Steep Slopes. Soil Science Society of America Journal 64 (5), 1759–1763. https://doi.org/10.2136/sssaj2000.6451759x.

Liu, Y., Dang, C., Yue, H., Lyu, C., Dang, X., 2021. Enhanced drought detection and monitoring using sun-induced chlorophyll fluorescence over Hulun Buir Grassland. China. Science of The Total Environment 770. https://doi.org/10.1016/j.scitotenv.2021.145271 145271.

Liu, Z., 2019. Soil Erosion Research based on Remote Sensing and GIS Technology in Central Yunnan Province. Yunnan Normal University.

Liu, Z., Zhang, J., Wang, J., 2020. Temporal and Spatial Variation of Soil Erosion in Central Yunnan Province, China. Applied Ecology and Environmental Research 18 (5), 6691–6712. https://doi.org/10.15666/aeer/1805_66916712.

Magesh, N.S., Chandrasekar, N., 2016. Assessment of soil erosion and sediment yield in the Tamiraparani sub-basin, South India, using an automated RUSLE-SY model. Environmental Earth Sciences 75 (16), 1208. https://doi.org/10.1007/s12665-016-6010-x.

Mathbout, S., Lopez-Bustins, J.A., Martin-Vide, J., Bech, J., Rodrigo, F. S., 2018. Spatial and temporal analysis of drought variability at several time scales in Syria during 1961–2012. Atmospheric Research 200, 153–168. https://doi.org/10.1016/j.atmosres.2017.09.016.

McCool, D.K., Brown, L.C., Foster, G.R., Mutchler, C.K., Meyer, L.D., 1987. Revised Slope Steepness Factor for the Universal Soil Loss Equation. Transactions of the ASAE 30 (5), 1387–1396. https://doi.org/10.13031/2013.30576.

McKee, T.B., Doesken, N.J., J, K, 1993. The relationship of drought frequency and duration to time scales, Proceedings of the 8th Conference on Applied Climatology. American Meteorological Society, Boston, MA.

Nepal, S., Tripathi, S., Adhikari, H., 2021. Geospatial approach to the risk assessment of climate-induced disasters (drought and erosion) and impacts on out-migration in Nepal. International Journal of Disaster Risk Reduction 59. https://doi.org/10.1016/j.ijdrr.2021.102241 102241.

Olorunfemi, I.E., Komolafe, A.A., Fasinmirin, J.T., Olufayo, A.A., Akande, S.O., 2020. A GIS-based assessment of the potential soil erosion and flood hazard zones in Ekiti State, Southwestern Nigeria

using integrated RUSLE and HAND models. CATENA 194. https://doi.org/10.1016/j.catena.2020.104725 104725.

Pal, S.C., Chakrabortty, R., 2019. Simulating the impact of climate change on soil erosion in sub-tropical monsoon dominated watershed based on RUSLE, SCS runoff and MIROC5 climatic model. Advances in Space Research 64 (2), 352–377. https://doi.org/10.1016/j.asr.2019.04.033.

Pearson, K., 1901. LIII. On lines and planes of closest fit to systems of points in space. The London, Edinburgh, and Dublin Philosophical Magazine and Journal of Science 2 (11), 559–572. https://doi.org/10.1080/14786440109462720.

Peng, S., Yang, K., Hong, L., Xu, Q., Huang, Y., 2018. Spatio-temporal evolution analysis of soil erosion based on USLE model in Dianchi Basin. Transactions of the Chinese Society of Agricultural Engineering 34(10), 138-146+305.

Phinzi, K., Ngetar, N.S., 2019. The assessment of water-borne erosion at catchment level using GIS-based RUSLE and remote sensing: A review. International Soil and Water Conservation Research 7 (1), 27–46. https://doi.org/10.1016/j.iswcr.2018.12.002.

Pickering, B.J., Duff, T.J., Baillie, C., Cawson, J.G., 2021. Darker, cooler, wetter: forest understories influence surface fuel moisture. Agricultural and Forest Meteorology 300. https://doi.org/10.1016/j.agrformet.2020.108311 108311.

Piyathilake, I., Udayakumara, E.P.N., Gunatilake, S.K., 2021. GIS and RS Based Soil Erosion Modelling in Sri Lanka: A Review. Journal of Agricultural Sciences 16 (1), 143–162. https://doi.org/10.4038/jas.v16i1.9192.

Prasannakumar, V., Vijith, H., Geetha, N., Shiny, R., 2011. Regional Scale Erosion Assessment of a Sub-tropical Highland Segment in the Western Ghats of Kerala. South India. Water Resources Management 25 (14), 3715–3727. https://doi.org/10.1007/s11269-011-9878-y.

Qin, W., Guo, Q., Cao, W., Yin, Z., Yan, Q., Shan, Z., Zheng, F., 2018. A new RUSLE slope length factor and its application to soil erosion assessment in a Loess Plateau watershed. Soil and Tillage Research 182, 10–24. https://doi.org/10.1016/j.still.2018.04.004.

Rahmati, O., Panahi, M., Kalantari, Z., Soltani, E., Falah, F., Dayal, K. S., Mohammadi, F., Deo, R.C., Tiefenbacher, J., Tien Bui, D., 2020. Capability and robustness of novel hybridized models used for drought hazard modeling in southeast Queensland. Australia. Science of The Total Environment 718. https://doi.org/10.1016/j.scitotenv.2019.134656 134656.

Rajbanshi, J., Bhattacharya, S., 2020. Assessment of soil erosion, sediment yield and basin specific controlling factors using RUSLE-SDR and PLSR approach in Konar river basin. India. Journal of Hydrology 587. https://doi.org/10.1016/j.jhydrol.2020.124935 124935.

Saaty, Thomas L., 1988. In: Mathematical Models for Decision Support. Springer Berlin Heidelberg, Berlin, Heidelberg, pp. 109–121. https://doi.org/10.1007/978-3-642-83555-1_5.

Safwan, M., Alaa, K., Omran, A., Quoc, B.P., Nguyen, T.T.L., Van, N.T., Duong, T.A., Endre, H., 2021. Predicting soil erosion hazard in Lattakia Governorate (W Syria). International Journal of Sediment Research 36 (2), 207–220. https://doi.org/10.1016/j.ijsrc.2020.06.005.

Santos, Celso Augusto Guimarães, Brasil Neto, Reginaldo Moura, Nascimento, Thiago Victor Medeiros do, Silva, Richarde Marques da, Mishra, Manoranjan, Frade, Tatiane Gomes, 2021. Geospatial drought severity analysis based on PERSIANN-CDR-estimated rainfall data for Odisha state in India (1983–2018). Science of The Total Environment 750, 141258. https://doi.org/10.1016/j.scitotenv.2020.141258.

Santra, A., Santra Mitra, S., 2020. Space-Time Drought Dynamics and Soil Erosion in Puruliya District of West Bengal, India: A Conceptual Design. Journal of the Indian Society of Remote Sensing 48 (8), 1191–1205. https://doi.org/10.1007/s12524-020-01147-y.

Shao, W., Kam, J., 2020. Retrospective and prospective evaluations of drought and flood. Science of The Total Environment 748. https://doi.org/10.1016/j.scitotenv.2020.141155 141155.

Shen, R., Huang, A., Li, B., Guo, J., 2019. Construction of a drought monitoring model using deep learning based on multi-source remote sensing data. International Journal of Applied Earth Observation and Geoinformation 79, 48–57. https://doi.org/10.1016/j.jag.2019.03.006.

Shi, D., 1996. Soil and Water Losses and Its Effects on Droughts and Floods in China. Journal of Natural Disasters 5 (02), 36–46.

Sidiropoulos, P., Dalezios, N.R., Loukas, A., Mylopoulos, N., Spiliotopoulos, M., Faraslis, I.N., Alpanakis, N., Sakellariou, S., 2021. Quantitative Classification of Desertification Severity for Degraded Aquifer Based on Remotely Sensed Drought Assessment. Hydrology 8 (1), 47. https://doi.org/10.3390/hydrology8010047.

Teng, H.-F., Hu, J., Zhou, Y., Zhou, L.-Q., Shi, Z., 2019. Modelling and mapping soil erosion potential in China. Journal of Integrative Agriculture 18 (2), 251–264. https://doi.org/10.1016/S2095-3119(18)62045-3.

Teng, H., 2017. Assimilating multi-source data to model and map potential soil loss in China. Zhejiang University.

Tian, P., Zhu, Z., Yue, Q., He, Y., Zhang, Z., Hao, F., Guo, W., Chen, L., Liu, M., 2021. Soil erosion assessment by RUSLE with improved P factor and its validation: Case study on mountainous and hilly areas of Hubei Province, China. International Soil and Water Conservation Research 9 (3), 433–444. https://doi.org/10.1016/j.iswcr.2021.04.007.

Tsegaye, L., Bharti, R., 2021. Soil erosion and sediment yield assessment using RUSLE and GIS-based approach in Anjeb watershed. Northwest Ethiopia. SN Applied Sciences 3 (5), 582. https://doi.org/10.1007/s42452-021-04564-x.

Vicente-Serrano, S.M., Beguería, S., López-Moreno, J.I., 2010. A Multiscalar Drought Index Sensitive to Global Warming: The Standardized Precipitation Evapotranspiration Index. Journal of Climate 23 (7), 1696–1718.

Wang, B., Bi, R., Chen, L., Jing, Y., 2019. Soil Erosion in Loess Area of the Upstream of the Hutuo River: Spatial Characteristics Based on USLE Model. Chinese Agricultural Science Bulletin 36 (7), 75–82.

Wang, J., Li, X., Christakos, G., Liao, Y., Zhang, T., Gu, X., Zheng, X., 2010. Geographical Detectors-Based Health Risk Assessment and its Application in the Neural Tube Defects Study of the Heshun Region, China. International Journal of Geographical Information Science 24 (1), 107–127. https://doi.org/10.1080/13658810802443457.

Wang, J., Zhu, X., Liu, X., Pan, Y., 2018. Research on agriculture drought monitoring method of Henan Province with multi-sources data. Remote Sensing for Land & Resources 30 (1), 180–186.

Wang, X., Yang, B., Li, G., 2020. Drought-induced tree growth decline in the desert margins of Northwestern China. Dendrochronologia 60. https://doi.org/10.1016/j.dendro.2020.125685 125685.

Wei, C., Wei, J., Kong, Q., Fan, D., Qiu, G., Feng, C., Li, F., Preis, S., Wei, C., 2020. Selection of optimum biological treatment for coking wastewater using analytic hierarchy process. Science of The Total Environment 742. https://doi.org/10.1016/j.scitotenv.2020.140400 140400.

Wischmeier, W.H., Smith, D.D., 1965. Predicting rainfall-erosion losses from cropland east of the Rocky Mountains: a guide to conservation planning. USDA Agricultural Handbook 282, 1–17.

WRB, 2014. The rules for classifying soils and creating map legends. World Reference Base for Soil Resources 2014: international soil classification system for naming soils and creating legends for soil maps. Food and Agriculture Organization of the United Nations, pp. 12–21.

Wu, Lei, Liu, Xia, Yang, Zhi, Chen, Junlai, Ma, Xiaoyi, 2021. Landscape scaling of different land-use types, geomorphological styles, vegetation regionalizations, and geographical zonings differs spatial erosion patterns in a large-scale ecological restoration watershed. Environmental Science and Pollution Research 28 (28), 38374–38392. https://doi.org/10.1007/s11356-021-13274-1.

Yang, Siyao, Meng, Dan, Gong, Huili, Li, Xiaojuan, Wu, Xinling, 2018. Soil Drought and Vegetation Response during 2001–2015 in North China Based on GLDAS and MODIS Data. Advances in Meteorology 2018, 1–14. https://doi.org/10.1155/2018/1818727.

Yao, Junqiang, Zhao, Yong, Chen, Yaning, Yu, Xiaojing, Zhang, Ruibo, 2018. Multi-scale assessments of droughts: A case study in Xinjiang, China. Science of the Total Environment 630, 444–452.

Yu, H., Li, L., Liu, Y., Li, J., 2019. Construction of Comprehensive Drought Monitoring Model in Jing-Jin-Ji Region Based on Multi-source Remote Sensing Data. Water 11 (5), 1077.

Yu, H., Wang, L., Wen, J., Yang, R., 2014. Study on spatial and temporal distribution of drought disaster in 500 years in Yunnan province. Journal of Arid Land Resources and Environment 28 (12), 38–44.

Xu, K., Zeng, H., Ren, J., Xie, J., Yang, Y., 2016. Spatial and temporal variations in vegetation cover in an eroded region of substropical red soil and its relationship with the impact of human activity. Acta Ecologica Sinica 36 (21), 6960–6968.

Yu, Y., 2020. Study of Comprehensive Drought Monitoring Model of Yunnan Province Based on Multi-source Remote Sensing Data. Yunnan Normal University.

Yu, Y., Wang, J., 2020. Applicability Evaluation of TRMM 3B43 Precipitation Data for Downscaling in Yunnan Province. Chinese Journal of Agrometeorology 41(09), 575-586.

Yu, Y., Wang, J., Cheng, F., Deng, H., Chen, S., 2020. Drought monitoring in Yunnan Province based on a TRMM precipitation product. Natural Hazards 104 (3), 2369–2387. https://doi.org/10.1007/s11069-020-04276-2.

Zhang, B., He, C., Burnham, M., Zhang, L., 2016. Evaluating the coupling effects of climate aridity and vegetation restoration on soil erosion over the Loess Plateau in China. Science of The Total Environment 539, 436–449. https://doi.org/10.1016/j.scitotenv.2015.08.132.

Zhang, H., 2020. The development characteristics of landslides and the disaster pregnant environment of the high incidence area in Yunnan Province. Yunnan University.

Zhang, J., Shen, R.p., Guo, J, 2017. A Study of Application of Different Data Mining methods in Integrated Drought Monitoring. Acta Agriculturae Universitatis Jiangxiensis 39 (5), 1047–1056.

Zhao, L., Qin, J., Sun, H., 2011. Research Progress in Soil Water Repellency. World Sci-Tech R & D 33(01), 58-64+102.

Zhao, Y., Huang, P., 2012. Yunnan Jianzai Nianjian (2010–2011). Yunnan Science and Technology Press, Kunming.

Zhao, Y., Huang, P., 2014. Yunnan Jianzai Nianjian (2012–2013). Yunnan Science and Technology Press, Kunming.

Zhao, Y., Huang, P., 2016. Yunnan Jianzai Nianjian (2014–2015). Yunnan Science and Technology Press, Kunming.

Zhao, Y., Liu, L., Kang, S., Ao, Y., Han, L., Ma, C., 2021. Quantitative Analysis of Factors Influencing Spatial Distribution of Soil Erosion Based on Geo-Detector Model under Diverse Geomorphological Types. Land 10 (6), 604. https://doi.org/10.3390/land10060604.

Zhou, G., Yang, Z., 2013. Summary on Natural Disasters in Yunnan in 2012 and Discussion on Disaster Reduction Measures. Journal of Catastrophology 28 (4), 132–138.